Manipulating the Fragmentation Patterns of Phosphopeptides via Gas-Phase Boron Derivatization: Determining Phosphorylation Sites in Peptides with Multiple Serines

Scott Gronert, Kathy H. Li, and Mizue Horiuchi
Department of Chemistry and Biochemistry, San Francisco State University, San Francisco, California, USA

Trivalent boron species readily react with protonated phosphopeptides to give addition products with the loss of boron ligands. In the present study, trimethoxyborane (TMB), diisopropoxymethylborane (DIPM), and diethylmethoxyborane (DEMB) were allowed to react with four phosphopeptides, VsSF, LSsF, LsGASA, and VSGAsA (lower-case s indicates phosphoserine). Each of the phosphopeptides contains one serine that is phosphorylated and one that is not. Under collision-activated dissociation (CAD) conditions, the boron-derivatized peptides give fragmentation patterns that differ significantly from that of the protonated phosphopeptide. The patterns vary, depending on the number of labile (i.e., alkoxy) ligands on the boron. In general, boron derivatization increases the yield of phosphate-containing sequence ions, but dramatic effects are only seen with certain reagent/peptide combinations. However, the suite of reagents provides a means of altering and increasing the information content of phosphopeptide CAD spectra. (J Am Soc Mass Spectrom 2005, 16, 1905–1914) © 2005 American Society for Mass Spectrometry

Phosphorylation is a critical post-translational modification in proteins and has been the subject of intense interest in recent years [1–4]. It is an important control mechanism of cellular activity and plays a variety of other roles in biological systems. Phosphorylation levels are often low, so highly sensitive analytical techniques, such as mass spectrometry, are needed [5]. Although mass analysis of the peptides derived from the digestion of phosphoproteins is a powerful tool for identifying phosphorylation sites [6–18], it gives ambiguous results if the peptide contains more than one of the commonly phosphorylated amino acids, serine, threonine, or tyrosine. Identification of the phosphorylation site in these cases requires fragmentation of the peptide and the CAD process with phosphopeptides is plagued by H_3PO_4 loss rather than sequence ion formation, which greatly complicates the analysis [19, 20]. However, electron-capture dissociation is less prone to this problem [14, 15, 18]. Recently we showed that treatment with trimethoxyborane (TMB) in the gas-phase before fragmentation has a strong influence on the breakdown of phosphopeptides and can lead to more fragments that retain the phosphate [21, 22]. As a result, boron derivatization provides a novel approach for gaining additional information about phosphorylation sites. More recently, others have used boron derivatization to analyze sugars [23, 24] and nucleotide [25].

In the present work, we begin with a computational study focused on the competition between H_3PO_4 loss and peptide cleavage in a model peptide, the N-methyl amide of Gs (lower-case s indicates phosphoserine). Next, experiments are presented that illustrate how the nature of the boron reagent as well as subtle variations in the phosphopeptide structure can have dramatic effects on the fragmentation behavior during CAD. The results suggest that derivatization experiments can be tailored to acquire the information needed to determine the phosphorylation site. For this study, we have focused on two very similar tetrapeptides, LSsF and VsSF that contain adjacent serines, one of which is phosphorylated. This situation provides a reasonably demanding test of a method's ability to identify a phosphorylation site. In addition, we have included two peptides from previous work, VSGAsA and LsGASA [22]. Three boron reagents have been used: trimethoxyborane (TMB), diisopropoxymethylborane (DIPM), and diethylmethoxyborane (DEMB). The major change across this series is the number of labile ligands (alkoxy) on the boron. This variation has an impact on the number of coordination sites that the boron has available for binding to the phosphopeptide. The data show that both the location of the phosphorylation site and the coordination state of the boron has a marked effect on the fragmentation pattern of the phosphopeptide.

Published online October 20, 2005

Address reprint requests to Dr. S. Gronert, Department of Chemistry and Biochemistry, San Francisco State University, 1600 Holloway Avenue, San Francisco, CA 94132, USA. E-mail: sgronert@sfsu.edu

1044-0305/05/$30.00
doi:10.1016/j.jasms.2005.07.018

Received May 24, 2005
Revised July 12, 2005
Accepted July 14, 2005

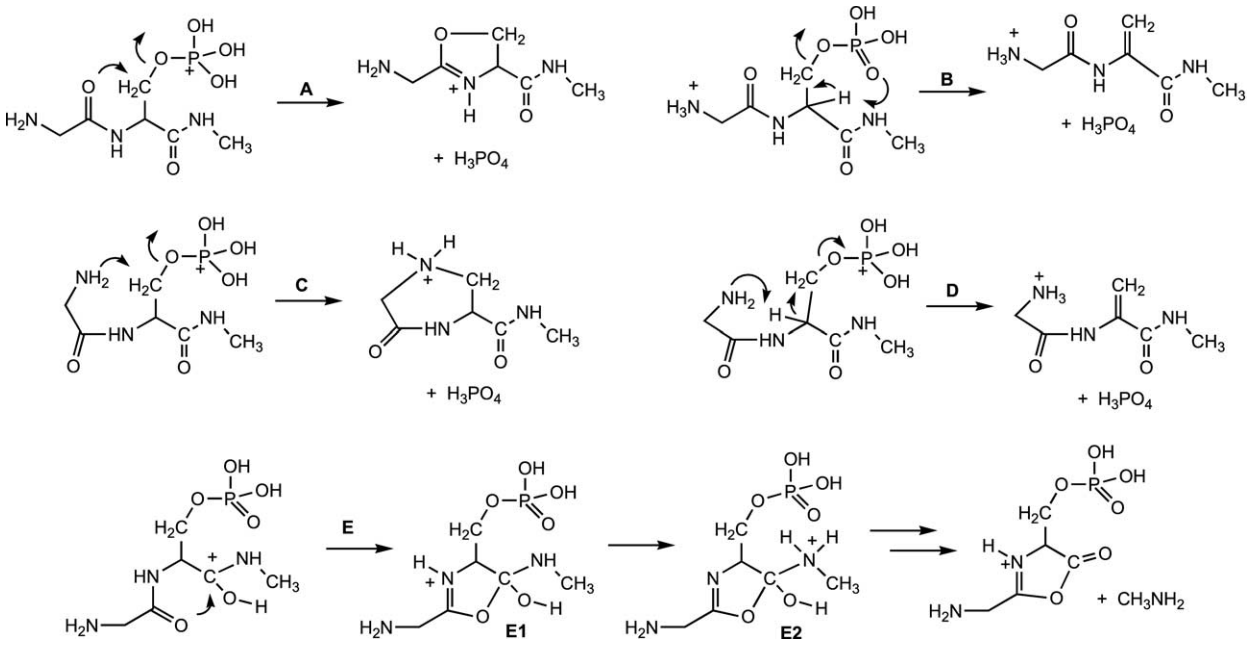

Scheme 1

Methods

All experiments were completed in a modified Finnigan-LCQ (San Jose, CA) quadrupole ion trap with an electrospray ionization (ESI) source. The instrument is equipped with an external gas manifold that allows reagents to be mixed into the helium buffer gas of the ion trap [26–28]. Liquid reagents are introduced into a measured, fast flow of helium by a syringe pump. We developed this approach a number of years ago and it provides a convenient method for studying gas-phase ion molecule reactions at near thermal energies [27].

The peptides were obtained from United Biochemical Technologies (Seattle, WA) and used without further purification. For the studies of acetylated peptides, 1 mL of the peptide solution (~ 0.1 mM in a 75/25 mix of CH_3OH/H_2O) was treated with 5 uL of acetic anhydride and allowed to react for 2 h. Typical conditions were used in the ESI source to generate the peptide ions. For the derivatization experiments, the external manifold was used to spike the helium buffer gas with the derivatization reagent. The peptide ion was isolated with a notched waveform and then held in the trap for a preset time delay to allow for reactions with the derivatization reagent. By varying the time delay and the derivatization reagent's partial pressure, the extent of reaction was conveniently controlled. The appropriate product ion was isolated by applying a notched waveform and then was subjected to CAD. This process was repeated until sequence ions were generated. Because the derivatization reagent is in the trap throughout the experiment, secondary reaction product ions are formed, but this problem can be minimized by careful choice of the time delays (typically 2 to 3 s for reactions and 30 ms for subsequent CAD activation) and reagent pressure. CAD spectra in the absence of the derivatization reagent were generated in the normal way. In general, final CAD voltages were adjusted to reduce the parent ion to ~ 25% relative to the base peak in the spectrum. Higher CAD voltages only had a minor effect on the observed spectra because the multi-collisional nature of CAD in the ion trap does not allow for excessive activation.

TMB, DIPM, DEMB, acetic anhydride, as well as the ESI solvents were obtained from commercial sources and used without further purification.

Calculations were completed with the Spartan02 [29] and Gaussian03 [30] quantum mechanical packages. Conformational searches were completed at the PM3 level using Spartan02. For the peptide models (Scheme **1**), the most stable conformations then were used for optimizations and subsequent frequency calculations at the HF/6-31 + G(d) level. All of the species in the study exhibited the proper number of imaginary frequencies. Next, optimizations were completed at the MP2/6-31 + G(d) level. Finally, single-point energies were calculated at the MP2/6-311 + G(d,p)//MP2/6-31 + G(d) level. Relative energies reported in Table 1 are at the MP2/6-311 + G(d,p) level corrected for zero-point vibrational energies (ZPE, HF values scaled by 0.9153 [31]. The transition-state on Pathway **D** proved to be exceptionally complex at the MP2 level. The HF transition-state collapsed to products at the MP2 level and, after extensive searches at the MP2 level, we were able to locate a species that involved an additional proton transfer component (protonated amide to phosphate). However, we were not able to get the species to fully converge and, therefore, we truncated the optimization at a point that appears to be close to the true transition-

Table 2. Reaction Energies with TMB: Z—H + $B(OCH_3)_3$ = > Z—$B(OCH_3)_2$ + CH_3OH

Z—H	B3LYP/6-311+G(d,p)[a]
H_3PO_4	−0.9
CH_3OH	0.0
CH_3NH_2	6.9
CH_3CO_2H	10.3
$CH_3C(O)NHCH_3$ (on N)	18.8
$CH_3C(O)NHCH_3$ (on O)	23.8

[a]Energies in kcal/mol corrected for ZPE (see text).

state. For the products from the reaction of TMB with sample functional groups (Table 2), optimizations were completed at the B3LYP/6-31 + G(d) level; the values in the table are at the B3LYP/6-311 + G(d,p) level corrected for B3LYP/6-31 + G(d) zero-point vibrational energies (scaled by 0.9806 [31]). The less computationally demanding B3LYP density functional theory (DFT) method could be used here because transition states are not involved (DFT is known to underestimate transition-state barriers in eliminations and related reactions [32]).

Results and Discussion

Computational Modeling

The key problem in the analysis of phosphopeptides via CAD is the facile loss of H_3PO_4. Clearly, low-energy pathways are available for this process that can compete with typical peptide backbone cleavages. To gain more insight into this issue, we have used computational methods to explore five reaction paths in a small phosphopeptide, the N-methyl amide of Gs. The pathways are illustrated in Scheme **1**. Paths **A** to **D** lead to H_3PO_4 loss, whereas Path **E** leads to amide bond cleavage. In Path **A**, a carbonyl acts as a nucleophile to displace a protonated phosphate. In Path **B**, an intramolecular elimination results in H_3PO_4 loss. Path **C** is like Path **A**, but the terminal amine acts as the nucleophile. In Path **D**, the terminal amine acts as a base to induce an elimination reaction similar to that in Path **B**. These two paths, **C** and **D**, are unique to peptides with a phosphoserine at position two. In Path **E**, we have only considered the two intermediates in the cyclization process shown in Scheme **1** [33].

Table 1. Relative energies of transition states and intermediates[a]

Pathway	Relative energy	Description
A	36.8	amide cyclization/H_3PO_4 loss
B	39.7	H_3PO_4 1,2-elimination
C	37.0	N-terminal cyclization/H_3PO_4 loss
D	37.6	N-terminal induced H_3PO_4 elimination
E1	30.5	b-ion formation intermediate 1
E2	35.6	b-ion formation intermediate 2

MP2/6-31 + G(d,p)//MP2/6-31 + G(d) level corrected for ZPE (see text).
[a]Energies in kcal/mol relative to reactant ion.

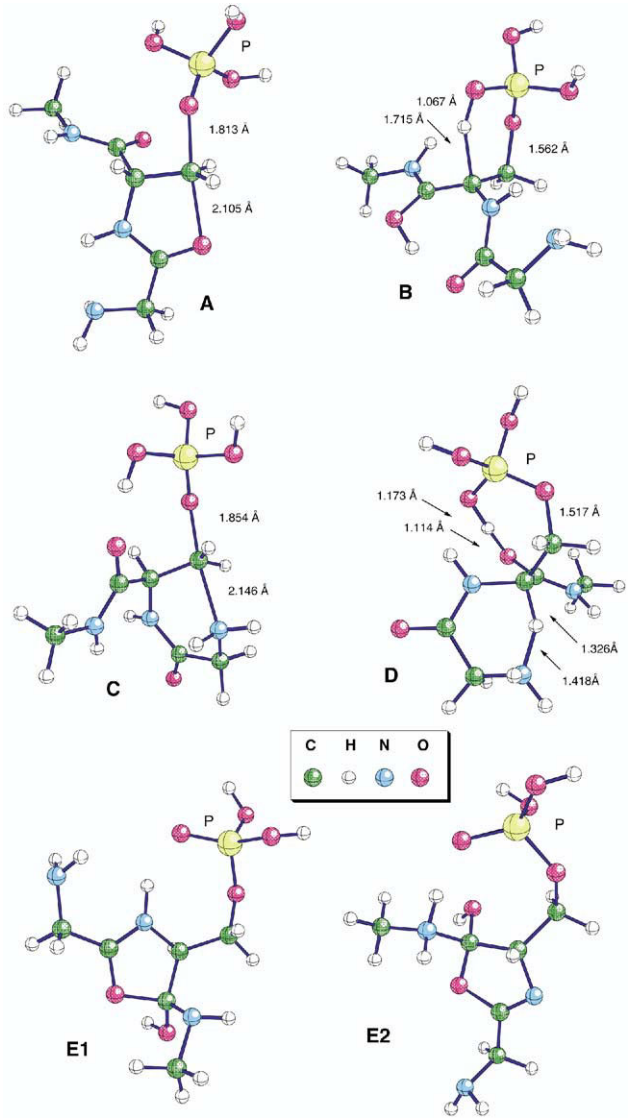

Figure 1. Structures of transition states for the loss of H_3PO_4 and the intermediates in b-ion formation from protonated glycylphosphoserine N-methyl amide (MP2/6-31 + G(d) level).

Computational data at the MP2/6-311 + G(d,p)//MP2/6-31 + G(d) level are listed in Table 1. Structures are shown in Figure 1. For Paths **A** to **D**, the key species are transition states, but for Path **E** the first and second intermediate have been used (**E1** and **E2**). Here, the path involves multiple proton transfers, which likely have small barriers relative to the intermediates. These proton transfers will be assisted by basic groups on a peptide chain and, therefore, cannot be realistically modeled by a species as small as a dipeptide. Consequently, we will assume that the energies required to reach these intermediates are rough approximations of the barriers on this pathway. Because we are only seeking a qualitative picture of the competing processes, this is a reasonable assumption. The transition-

state on Pathway **D** is unusually complex and involves two proton transfers (H_α to NH_2 and protonated amide to phosphate) along with the H_3PO_4 expulsion. In this case, the MP2 structure is only an approximate transition-state (see the Methods section). The computational data in Table 1 indicate that the four paths to H_3PO_4 expulsion have fairly similar barriers and are likely to compete. Although the two intermediates on the b-ion formation on Pathway (**E**) are lower in energy than the H_3PO_4 expulsion transition states, it is possible/likely that the proton transfer transition states separating them are close to the energies of the other transition states (**A** to **D**). Moreover, this pathway is entropically less favorable because it involves multiple transition states on the way to products. A survey of all the transition states on the surface as well as the dynamics of the processes are well beyond the scope of the present work and as noted above, could not be directly extrapolated from a dipeptide to a larger peptide. Nonetheless, the results highlight the fact that these reaction surfaces have many paths with similar barriers. Most importantly, H_3PO_4 loss can occur simultaneously by multiple paths, particularly in systems where the phosphoserine is at position 2 in the peptide.

To analyze the effects of boron derivatization on fragmentation behavior, it is useful to consider the thermodynamics of the reactions of a phosphopeptide with a boron reagent. The boron derivatization reactions generally involve the replacement of an alkoxy ligand on boron with a nucleophilic group from the peptide. The likely nucleophiles on the peptides in this study are a hydroxy group (serine side-chain), a phosphate, an amino group (N-terminus), a carboxyl group (C-terminus), or an amide group (N or O). We have used calculations at the B3LYP/6-311 + G(d,p)//B3LYP/6-31 + G(d) level to explore the energetics of the processes. Data are given in Table 2 for the reactions of TMB with model nucleophiles: methanol (identity reaction), phosphoric acid, methylamine, acetic acid, and N-methylacetamide (eq 1). The results indicate that the favored peptide nucleophiles are hydroxy groups and phosphates. Reactions with amino or carboxyl groups are much less favorable. In fact, they are predicted to be endothermic in the model systems, but could be driven by collisional activation. Reactions on either the nitrogen or oxygen of an amide are predicted to be the least favorable. Therefore, the modeling suggests that there is a thermodynamic preference for the boron reagents to react with hydroxy and phosphate groups, if available, before reacting with amino, carboxyl, or amide groups. This result is consistent with our observation that TMB exhibits a preference for reactions with phosphate groups. We cannot directly investigate the kinetics of the reactions computationally using these model systems because they lack the additional proton donors/acceptors found in a peptide, which could play a pivotal role in protonating the departing boron ligand. Nonetheless, the thermodynamic data provide useful insights into the derivatization process.

$$Z - H + B(OCH_3)_3 \rightarrow Z - B(OCH_3)_2 + CH_3OH \qquad (1)$$

$$ZH = H_3PO_4,\ CH_3OH,\ CH_3NH_2,\ CH_3CO_2H,\ CH_3C(O)NHCH_3$$

VsSF

In this peptide, the phosphate is adjacent to the N-terminal residue. When the protonated phosphopeptide is subjected to fragmentation conditions in a quadrupole ion trap, the spectrum is dominated by the loss of H_3PO_4 (Figure 2a). The only other significant fragment corresponds to the loss of H_2O. This represents the worst case where no phosphate-containing sequence ions are formed during CAD and no information about the site of phosphorylation is obtained. The facile loss of H_3PO_4 is likely related to the location of the phosphoserine. In position 2, the phosphoserine is susceptible to intramolecular reactions with the N-terminal amino group. Attack either at the α-hydrogen or the side-chain carbon of the phosphoserine (to give dehydroalanine or a cyclic amine, respectively) involves a favorable six-membered ring transition-state (Paths **C** and **D** in Scheme **1**). The complete absence of phosphate-containing sequence ions suggests that the processes in Scheme **2**, along with Paths **A** and **B** (Scheme **1**), occur much more readily than backbone cleavages in this peptide.

When treated with TMB, boron addition with loss of two CH_3OH molecules is observed. CAD of this ion leads to the loss of the third CH_3OH molecule (Scheme **3**) to give an ion with an *m/z* value that is eight units greater than the parent ion (^{11}B containing ions). This pattern is the same one seen in our earlier work [22], and CAD on the "+8" ions leads to a breakdown of the peptide. For VsSF, CAD of the boron derivatized ion leads to the spectrum in Figure 2b. The impact is dramatic and H_3PO_4 loss is almost completely inhibited. Instead, a b_3 ion that retains the boron modification dominates the spectrum. Further CAD on this ion does not lead to an ion that would reveal the site of phosphorylation (e.g., a b_2 ion). Instead H_3PO_4 and small molecule loss (e.g., CO) are observed. Although boron derivatization helps retain the phosphate in this case, it does not provide the information needed to unambiguously assign the site (i.e., produce a sequence ion which retains the phosphorylated serine, but has lost the other serine). Recognizing that the N-terminal amine could be the problem, we treated the peptide with acetic anhydride to convert it to its N-acetyl amide. CAD of the resulting peptide (no boron derivatization) gives a more complex spectrum that exhibits combinations of H_3PO_4, H_2O, and $CH_2 = C = O$ loss (Figure 2c). In addition, relatively weak signals are seen for y_3, b_3, and $b_3 - H_3PO_4$ ions. Finally, a very small peak for a phosphate-retaining b_2 ion is observed (1% relative to

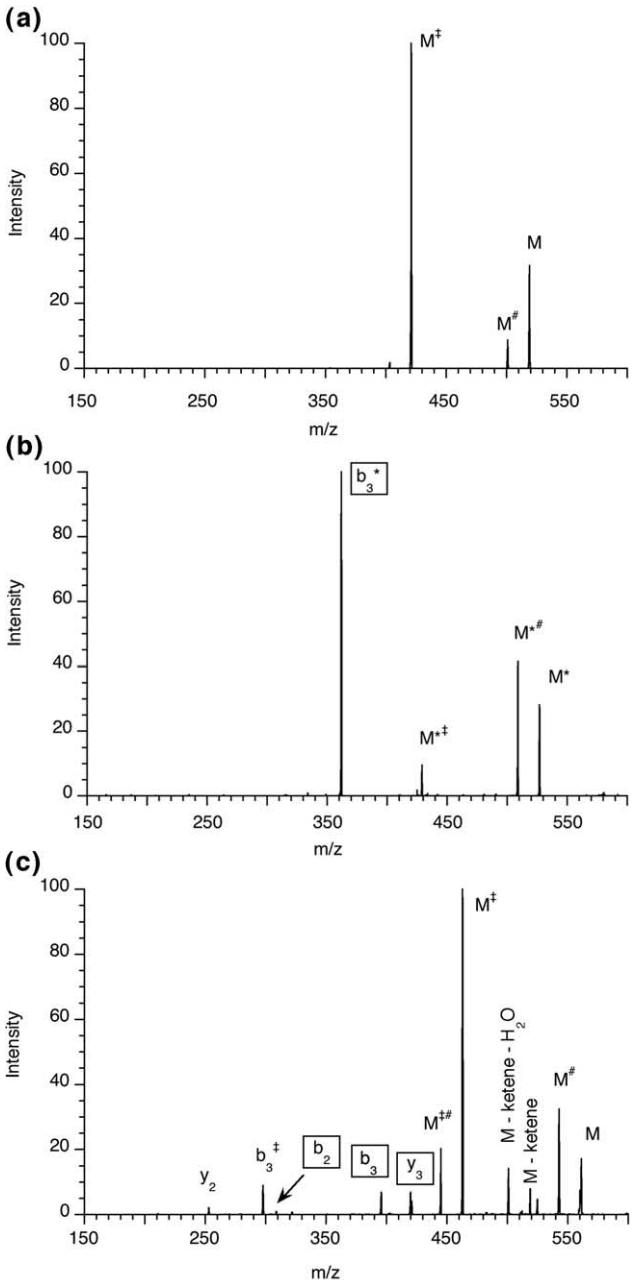

Figure 2. Spectra for VsSF and derivatives. M represents protonated peptide. The asterisk symbol indicates boron-containing ion. Products that have lost H_3PO_4 are designated with the double dagger symbol and those that have lost H_2O are designated with the pound symbol. Boxed labels are for phosphate-containing sequence ions. (**a**) CAD spectrum of protonated VsSF. (**b**) CAD spectrum of protonated TMB-derivatized VsSF. (**c**) CAD spectrum of protonated N-acetyl-VsSF.

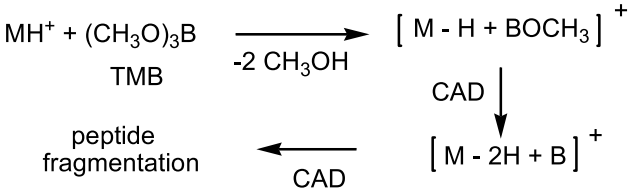

Scheme 3

H_3PO_4 loss). This ion definitively identifies the phosphorylation site. Nonetheless, the spectrum indicates that N-acetylation offers only limited protection against H_3PO_4 expulsion in this case. As a result, Pathways **A** or **B** (Scheme **1**) must be viable and active with this peptide. However, the reduction in H_3PO_4 loss seen in the acetylated peptide suggests that Pathways **C** or **D** are playing significant roles in the fragmentation of the parent peptide. When the protonated, acetylated peptide is treated with TMB before CAD, the spectrum (not shown) shows a mixture of H_3PO_4, H_2O, and CO loss. The only major sequence ion corresponds to a y_3 ion retaining the phosphate and boron. Interestingly, the N-acetylation alters the nature of fragments from the boron-derivatized peptide. Instead of forming N-terminal ions (b_3, see Figure 2b), C-terminal ions (y_3) are formed from the acetylated peptide. This result suggests that the bulk of boron derivatization has also shifted from the N-terminus to the C-terminus in response to acetylation. As noted above, amides have a low affinity for TMB, so it is not surprising that reaction would shift towards the C-terminus in the N-acetylated peptide. In any case, the combination of acetylation and TMB derivatization does not yield any definitive information concerning the site of phosphorylation in VsSF.

When treated with DIMB, protonated VsSF undergoes addition followed by the loss of two $(CH_3)_2CHOH$ molecules to give an ion whose *m/z* value is 24 units greater than the parent ion. CAD of the "+24" ion does not lead to the loss of the last boron ligand (CH_3), but results in a breakdown of the phosphopeptide (Scheme **4**). In this case, the boron reagent only has two labile ligands (alkoxy groups) so it retains one of its ligands during the fragmentation of the peptide. As a result, the boron has one less site available for coordinating to the phosphopeptide. CAD of this ion leads mainly to the loss of H_3PO_4 and gives a spectrum (not shown) that is fairly similar to that obtained for the underivatized ion (Figure 2a). The only significant difference is a very small signal for a derivatized b_3 ion. Apparently, the

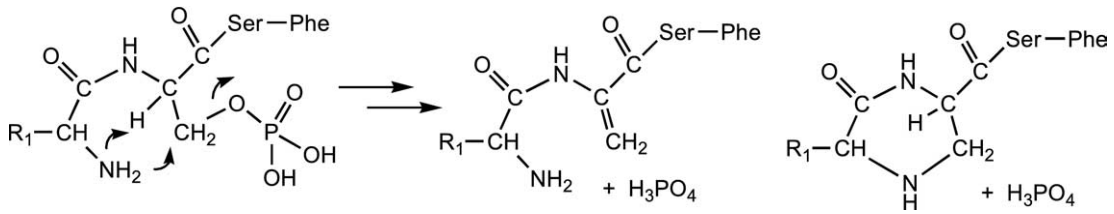

Scheme 2

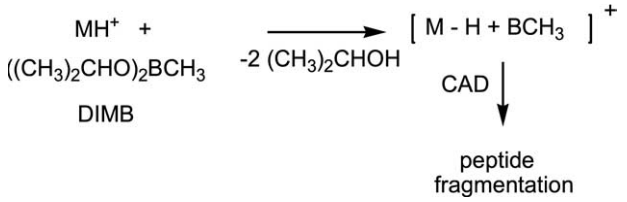

Scheme 4

presence of only two ligand exchange sites on the boron reagent reduces its ability to retain the phosphate group in this peptide.

The information from the computational modeling (see above) helps to rationalize the results with DIMB. If the reagent preferentially reacts with the hydroxy and phosphate groups on VsSF, it will leave the N-terminal amino group free to engage in the processes outlined in Scheme **2**. After the derivatization, the phosphate would be tethered to the boron, but the boron–phosphate bond is relatively labile and could breakdown if the bond between the serine and phosphate were cleaved (i.e., Scheme **2**). These results suggest that the third coordination site available in $(CH_3O)_3B$ allows it to sequester the N-terminal amino group and, therefore, prevents H_3PO_4 expulsion in this peptide.

When treated with DEMB, protonated VsSF yields two abundant derivatization ions corresponding to addition followed by the loss of CH_3OH ("+68" ion) or the loss of CH_3OH and CH_3CH_3 ("+38" ion). Both of these ions lead mainly to peptide fragmentation when subjected to CAD (Scheme **5**). The "+68" ion involves the loss of a single ligand from the boron and during CAD gives a high yield of H_3PO_4 loss as well as the loss of H_3PO_4 along with the boron group (spectrum not shown). The latter ion is consistent with the boron reagent bonding only to the phosphate group of the peptide. The "+38" ion results from the boron losing two ligands, and it gives H_3PO_4 loss as its major CAD product (spectrum not shown). The loss pattern is similar to that observed with DIMB, a reagent where the boron also loses two ligands before the peptide backbone breaks. It is interesting to note that although the "+68" and "+38" ions would seemingly be on the same fragmentation pathway (i.e., the "+68" ion leads to the "+38" ion), they give unrelated CAD spectra.

LSsF

When protonated LSsF is subjected to CAD, it gives a rich spectrum (Figure 3a). Although the loss of H_3PO_4 dominates, significant signals are seen for b_3 and y_2 ions as well as a y_2 ion that has lost H_3PO_4. The y_2 ion is noteworthy because it includes the phosphate but not the adjacent serine at position 2 of the chain. Therefore, this ion definitively indicates that the phosphate is at position 3 in the peptide. When treated with TMB, addition with the loss of two CH_3OH molecules is observed. CAD causes the loss of the third CH_3OH molecule and subsequent CAD causes the breakdown of the peptide (Scheme **3**). The CAD spectrum of the boron-derivatized peptide is simplified and is dominated by H_3PO_4 loss (Figure 3b). Along with H_2O loss, there is also a significant signal for the loss of H_2O and CO. Here, the TMB derivatization has the opposite effect—it seemingly promotes the loss of H_3PO_4. This reversal of effect is particularly striking given that the two peptides, LSsF and VsSF, are very similar in structure. The most likely explanation is that the boron derivatization impedes the backbone breakdown processes and therefore H_3PO_4 loss is more common than sequence ion formation.

Treatment with DIMB yields the reactivity pattern shown in Scheme **4**. When the "+24" ion is subjected to CAD, a rich spectrum results (Figure 3c). The strongest signal is for H_3PO_4 loss, but significant signals are also seen for a derivatized b_3 ion as well as a y_2 ion that has lost the boron group. Again, the spectrum provides useful information (i.e., the y_2 ion) for identifying the site of phosphorylation. Treatment with DEMB follows the pattern in Scheme **5** and produces a "+68" and "+38" ion. The "+68" ion gives a CAD spectrum with many peaks, the largest being for the loss of H_3PO_4, H_2O, and the boron group. There are significant derivatized sequence ions, including b_3, y_2, and b_2 ions. There is also a strong signal for a y_2 ion missing the phosphate group. The "+38" ions give a CAD spectrum that is dominated by a y_2 ion lacking the boron group. The intensity of this ion is striking in this spectrum and as noted above, it is critical in determining the site of phosphorylation (Figure 3d). Here, apparently the boron reagent is not intimately involved with the phosphate (it is not retained in the y_2 ion) but, instead, promotes backbone cleavage. In addition, there is a signal for a derivatized b_3 ion in the CAD spectrum of the "+38" ion. As in the previous peptide, there is a marked difference between the CAD spectra for the "+68" and "+38" ions. Again there are similarities in the loss patterns for the two systems that involve the loss of two boron ligands, the "+24" from DIMB and the "+38" ions from DEMB.

Other Peptides

In VsSF and LSsF, the choice of the boron reagent was critical in determining the information content of the CAD spectra. In each case, one of the three boron reagents was capable of suppressing H_3PO_4 loss and yielding CAD spectra with strong signals for sequence

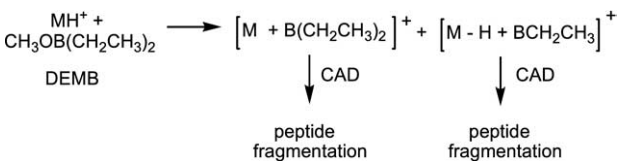

Scheme 5

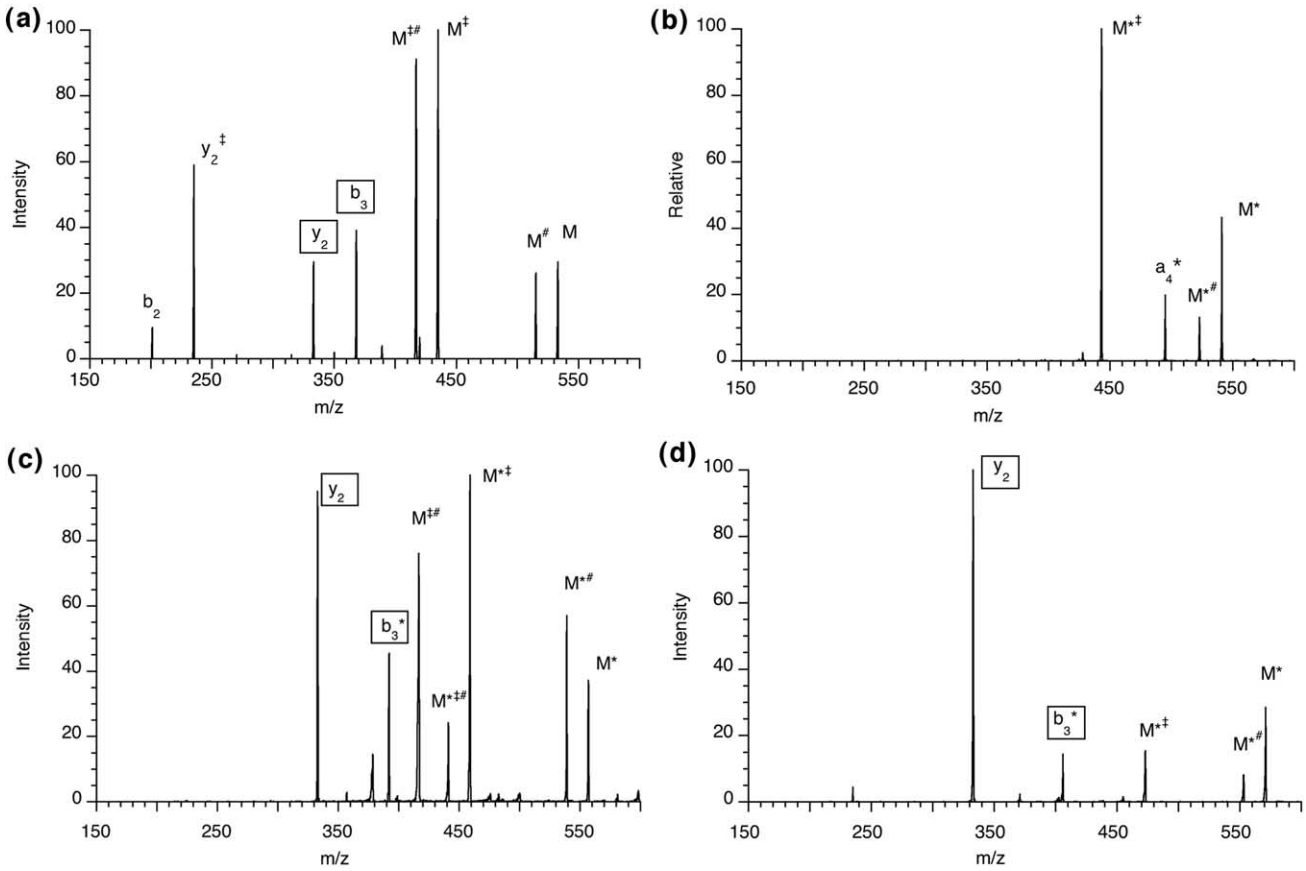

Figure 3. Spectra for LSsF and derivatives. M represents protonated peptide. The asterisk symbol indicates boron-containing ion. Products that have lost H_3PO_4 are designated with the double dagger symbol and those that have lost H_2O are designated with the pound symbol. Boxed labels are for phosphate-containing sequence ions. (**a**) CAD spectrum of protonated LSsF. (**b**) CAD spectrum of protonated TMB-derivatized LSsF. (**c**) CAD spectrum of protonated DIMB-derivatized LSsF. (**d**) CAD spectrum of protonated DEMB-derivatized LSsF ("+38" ion).

ions. To test the generality of the reagents, we have considered two other phosphopeptides that contain a phosphorylated and unphosphorylated serine, LsGASA and VSGAsA [22].

The CAD spectrum of protonated LsGASA is relatively simple (not shown) and is dominated by the loss of H_3PO_4. The sequence ions in the spectrum, b_5 and b_4, have intensities of 7 and 13%, respectively, relative to the signal for H_3PO_4 loss. Although the phosphorylated serine is in position 2 in this peptide, it seems to be somewhat less susceptible to the H_3PO_4 loss pathways shown in Scheme **2**. Nonetheless, the signals for the sequence ions are relatively weak. When treated with TMB before fragmentation, the intensities of the sequence ions are greatly reduced and the signals for the peptide losing H_2O and losing H_3PO_4 dominate the spectrum. Treatment with DIMB before fragmentation causes a dramatic change in the final CAD spectrum (Figure 4a). The loss of H_3PO_4 is greatly reduced. The dominant peak is for H_2O loss, but strong signals appear for (b_4 + H_2O) ions, with (*m/z* 451) and without (*m/z* 427) the boron group. These ions are useful in identifying the site of phosphorylation because they retain the phosphate but have lost the second serine residue. Here, the boron derivatization has opened up a new fragmentation pathway that was not observed in the parent peptide. Because the majority of the (b_4 + H_2O) ions lack the boron group, apparently the boron reagent is most often or most strongly interacting with the serine at position 5, which is lost during this fragmentation. Moreover, it appears to be assisting the cleavage of the bond between residues 4 and 5. Treatment with DEMB ("+68" ion) before fragmentation does not have a positive effect on the CAD spectrum (not shown). The loss of H_3PO_4 dominates and the sequence ions have relative intensities of 10% or less. As with LSsF, one of the boron reagents is capable of greatly enhancing the information content of the phosphopeptide's CAD spectrum.

In the CAD spectrum of protonated VSGAsA (not shown), H_3PO_4 loss dominates and there are weak signals (<10%) for sequence ions (b_5, b_4, and y_4). Treatment with TMB before fragmentation does not suppress H_3PO_4 loss and offers only a modest increase in the intensities of sequence ions. The same is true for treatment with DIMB. However, derivatization with

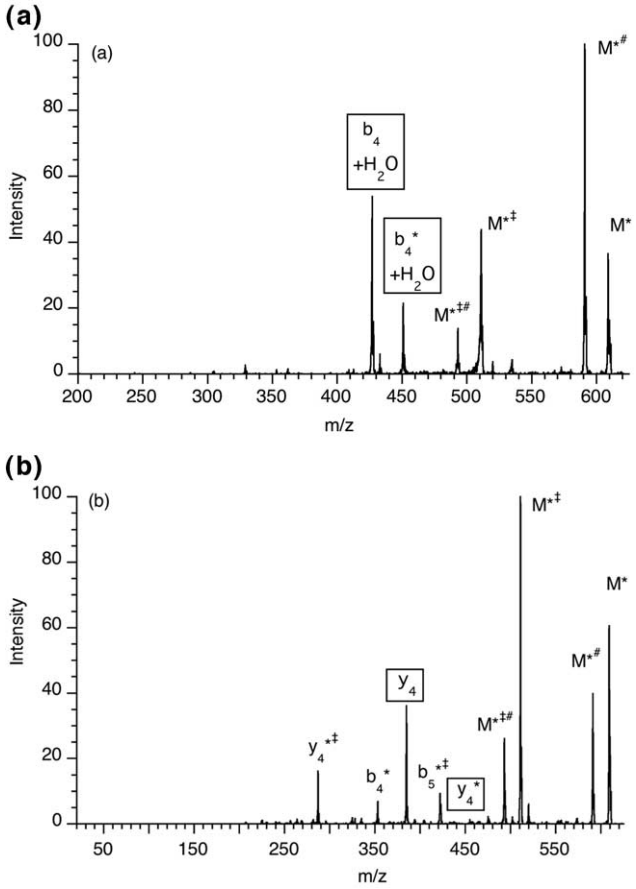

Figure 4. Spectra for LsGASA and VSGAsA derivatives. M represents protonated peptide. The asterisk symbol indicates boron-containing ion. Products that have lost H_3PO_4 are designated with the double dagger symbol and those that have lost H_2O are designated with the pound symbol. Boxed labels are for phosphate-containing sequence ions. (**a**) CAD of protonated DIMB-derivatized LsGASA ("+68" ion). (**b**) CAD spectrum of protonated DEMB-derivatized VSGAsA ("+38" ion).

DEMB ("+38" ion) has a major impact on the formation of sequence ions (Figure 4b). Specifically, a strong signal (36% relative to H_3PO_4 loss) is observed for a y_4 ion lacking the boron group. This ion is valuable because it retains the phosphate but only has one serine. The absence of the boron in this fragment ion suggests that its parent ion was derivatized on the N-terminus rather than near the phosphate. Support for this conjecture can be found in the b_4 ions in the spectrum, which are relatively weak, but do retain the boron.

Efficacy of the Method

In each of the four peptides in this study, boron derivatization altered the fragmentation spectra of the phosphopeptides and led to CAD spectra with greater relative intensities of sequence ions. The boron derivatization appears to have several modes of action in the altering the fragmentation behavior. It can (1) suppress H_3PO_4 loss by coordination to the phosphate group or an active nucleophile in the peptide, (2) open up new fragmentation pathways by inducing peptide bond cleavages, or (3) suppress peptide bond cleavages by changing the peptide conformation or sequestering a nucleophilic group. Given the complexity of the systems, it is difficult to predict how the boron reagent will affect the fragmentation pattern of any particular peptide. However, the ability to vary the number of labile ligands on the boron offers flexibility and the possibility of "tuning" the reagent to give the desired effect. Table 3 provides a summary of the results with the four peptides. The data confirm that the derivatization generally inhibits H_3PO_4 loss. More importantly, derivatization leads to a greater yield of sequence ions. In three peptides, boron derivatization causes a marked increase (3- to 9-fold) in the relative abundance of critical sequence ions (i.e., those giving definitive phosphorylation site information). In one peptide, VsSF, no critical sequence ions are generated with or without the boron derivatization; however, N-acetylation of this peptide led to a small signal of a diagnostic ion. It is disappointing that boron derivatization did not materially improve the information content of the VsSF spectra, but this peptide is a challenging case. Nonetheless, the results indicate that boron derivatization is a viable approach for modifying the nature and quality of the information generated in the CAD spectra of phosphorylated peptides.

Table 3. Percent yields of ions in CAD spectra of phosphorylated peptides

Peptide	Derivatization reagent	H_3PO_4 loss[a]	Sequence ions[b]	Critical sequence ions[c]
VsSF	None	91	0	0
	TMB	6	67	0
	DIMB	70	1	0
	DEMB (+68)	94	0	0
	DEMB (+38)	70	0	0
LSsF	None	69	23	8
	TMB	74	1	0
	DIMB	30	35	**24**
	DEMB (+68)	70	18	6
	DEMB (+38)	13	81	**72**
LsGASA	None	74	16	9
	TMB	74	7	4
	DIMB	23	35	**32**
	DEMB (+68)	68	11	3
	DEMB (+38)[d]			
VSGAsA	None	85	10	4
	TMB	66	16	**7**
	DIMB	75	9	5
	DEMB (+68)[d]			
	DEMB (+38)	63	20	**14**

[a]Total yield of ions lacking phosphate group.
[b]Total yield of sequence ions retaining the phosphate group.
[c]Total yield of sequence ions containing one serine and retaining the phosphate group. Bold values indicate higher yield than underivatized peptide.
[d]Ion was formed in low yield during initial reaction. No CAD spectra were obtained.

Conclusions

Gas-phase boron derivatization has a large impact on the fragmentation behavior of phosphopeptides and can lead to greater phosphate retention and to spectra with added information content. The substitution pattern of the boron reagent plays a role and the three reagents examined in this study led to different fragmentation patterns that provided varying types of sequence data. Although it is not possible to a priori choose the best reagent for a particular peptide, the suite of reagents studied here provides a means of increasing phosphate retention and, in most cases, significantly enhancing the signals of key sequence ions. Moreover, by altering the CAD patterns, the boron derivatization provides a relatively general means of increasing the sequence information available from fragmentation experiments. Additional studies focused on the scope and limitations of the method are underway.

Acknowledgments

The authors gratefully acknowledge support from the National Institutes of Health (NIH MBRS SCORE 5 SO6 GM52588).

References

1. Pawson, T.; Scott, J. D. Signaling through Scaffold, Anchoring, and Adaptor Proteins. *Science* **1997,** *278,* 2075.
2. Hubbard, M. J.; Cohen, P. On Target with a New Mechanism for the Regulation of Protein-Phosphorylation. *Trends Biochem. Sci.* **1993,** *18,* 172.
3. Hunter, T. Signaling—2000 and Beyond. *Cell* **2000,** *100,* 113.
4. Marks, F., Ed. *Protein Phosphorylation*; VCH: Weinheim, 1996.
5. Areces, L. B.; Matafora, V.; Bachi, A. Analysis of Protein Phosphorylation by Mass Spectrometry. *Eur. J. Mass Spectrom.* 2004, 10, 383.
6. Flora, J. W.; Muddiman, D. C. Gas-Phase Ion Unimolecular Dissociation for Rapid Phosphopeptide Mapping by IRMPD in a Penning Ion Trap: An Energetically Favored Process. *J. Am. Chem. Soc.* **2002,** *124,* 6546.
7. Ruijtenbeek, R.; Versluis, C.; Heck, A. J. R.; Redegeld, F. A. M.; Nijkamp, F. P.; Liskamp, R. M. J. Characterization of a Phosphorylated Peptide and Peptoid and Peptoid-Peptide Hybrids by Mass Spectrometry. *J. Mass Spectrom.* **2002,** *37,* 47.
8. Moyer, S. C.; Cotter, R. J.; Woods, A. S. Fragmentation of Phosphopeptides by Atmospheric Pressure MALDI and ESI/Ion Trap Mass Spectrometry. *J. Am. Soc. Mass Spectrom.* **2002,** *13,* 274.
9. Bennett, K. L.; Stensballe, A.; Podtelejnikov, A. V.; Moniatte, M.; Jensen, O. N. Phosphopeptide Detection and Sequencing by Matrix-Assisted Laser Desorption/Ionization Quadrupole Time-of-Flight Tandem Mass Spectrometry. *J. Mass Spectrom.* **2002,** *37,* 179.
10. Talbo, G. H.; Suckau, D.; Malkoski, M.; Reynolds, E. C. MALDI-PSD-MS Analysis of the Phosphorylation Sites of Caseinomacropeptide. *Peptides* **2001,** *22,* 1093.
11. Kinumi, T.; Niwa, H.; Matsumoto, H. Phosphopeptide Sequencing by In-Source Decay Spectrum in Delayed Extraction Matrix-Assisted Laser Desorption Ionization Time-of-Flight Mass Spectrometry. *Anal. Biochem.* **2000,** *277,* 177.
12. Tholey, A.; Reed, J.; Lehmann, W. D. Electrospray Tandem Mass Spectrometric Studies of Phosphopeptides and Phosphopeptide Analogs. *J. Mass Spectrom.* **1999,** *34,* 117.
13. Cao, P.; Stults, J. T. Phosphopeptide Analysis by On-Line Immobilized Metal-Ion Affinity Chromatography-Capillary Electrophoresis-Electrospray Ionization Mass Spectrometry. *J. Chromatogr. A* **1999,** *853,* 225.
14. Shi, S. D. H.; Hemling, M. E.; Carr, S. A.; Horn, D. M.; Lindh, I.; McLafferty, F. W. Phosphopeptide/Phosphoprotein Mapping by Electron Capture Dissociation Mass Spectrometry. *Anal. Chem.* **2001,** *73,* 19.
15. Stensballe, A.; Jensen, O. N.; Olsen, J. V.; Haselmann, K. F.; Zubarev, R. A. Electron Capture Dissociation of Singly and Multiply Phosphorylated Peptides. *Rapid Commun. Mass Spectrom.* **2000,** *14,* 1793.
16. Oda, Y.; Nagasu, T.; Chait, B. T. Enrichment Analysis of Phosphorylated Proteins as a Tool for Probing the Phosphoproteome. *Nat. Biotechnol.* **2001,** *19,* 379.
17. Zhou, H.; Watts, J. D.; Aebersold, R. A Systematic Approach to the Analysis of Protein Phosphorylation. *Nat. Biotechnol.* **2001,** *19,* 375.
18. Chalmers, M. J.; Hakansson, K.; Johnson, R.; Smith, R.; Shen, J.; Emmett, M.; Marshall, A. Protein Kinase a Phosphorylation Characterized by Tandem Fourier Transform Ion Cyclotron Resonance Mass Spectrometry. *Proteomics* **2004,** *4,* 970.
19. Kassel, D. B.; Blackborn, R. K.; Antonsson, B.In *Mass Spectrometry of Biological Materials*; Larsen, B. S., McEwen, C. N., Eds.; Dekker: New York, 1998; pp 137.
20. Dass, C. In *Mass Spectrometry of Biological Materials*; Larsen, B. S., McEwen, C. N., Eds.; Dekker: New York, 1998; pp 247.
21. Gronert, S.; Huang, R.; O'Hair, R. A. J. Salt Bridge Structures in the Gas Phase. *Proceedings of the 49th American Society for Mass Spectrometry Conference*; Chicago, IL, 2001.
22. Gronert, S.; Huang, R.; Li, K. H. Gas Phase Derivatization in Peptide Analysis I: The Utility of Trimethyl Borate in Identifying Phosphorylation Sites. *Int. J. Mass Spectrom.* **2004,** *231,* 179.
23. Leavell, M. D.; Kruppa, G. H.; Leary, J. A. Determination of Phosphate Position in Hexose Monosaccharides Using an FTICR Mass Spectrometer: Ion/Molecule Reactions, Labeling Studies, and Dissociation Mechanisms. *Int. J. Mass Spectrom.* **2003,** *222,* 135.
24. Leavell, M. D.; Kruppa, G. H.; Leary, J. A. Analysis of Phosphate Position in Hexose Monosaccharides Using Ion-Molecule Reactions and SORI-CID on an FT-ICR Mass Spectrometer. *Anal. Chem.* **2002,** *74,* 2608.
25. Vrkic, A. K.; O'Hair, R. A. J. Gas-Phase Ion Chemistry of Biomolecules Part XXXIV. Gas Phase Reactions of Trimethyl Borate with the [M − H](−) Ions of Nucleotides and Their Noncovalent Homo- and Heterodimer Complexes. *Aust. J. Chem.* **2003,** *56,* 389.
26. Gronert, S. Quadrupole Ion Trap Studies of Fundamental Organic Reactions. *Mass Spectrom. Rev.* **2005,** *24,* 100.
27. Gronert, S. Estimation of Effective Ion Temperatures in a Quadrupole Ion Trap. *J. Am. Soc. Mass Spectrom.* **1998,** *9,* 845.
28. Flores, A. E.; Gronert, S. The Gas-Phase Reactions of Dianions with Alkyl Bromides: Direct Identification of S_N2 and E2 Products. *J. Am. Chem. Soc.* **1999,** *121,* 2627.
29. Johnson, J. A.; Deppmeir, B. J.; Driessen, A. J.; Hehre, W. J.; Klunzinger, P. E.; Pham, I. N.; Watnabe, M. *Spartan 02 v1.0.7*; Wavefunction, Inc.: Irvine, CA, 2002.
30. Frisch, M. J.; Trucks, G. W.; Schlegel, H. B.; Scuseria, G. E.; Robb, M. A.; Cheeseman, J. R.; Montgomery, J. A.; Vreven, T.; Kudin, K. N.; Burant, J. C.; Millam, J. M.; Iyengar, S. S.; Tomasi, J.; Barone, V.; Mennucci, B.; Cossi, M.; Scalmani, G.; Rega, N.; Petersson, G. A.; Nakatsuji, H.; Hada, M.; Ehara, M.; Toyota, K.; Fukuda, R.; Hasegawa, J.; Ishida, M.; Nakajima, T.; Honda, Y.; Kitao, O.; Nakai, H.; Klene, M.; Li, X.; Knox, J. E.; Hratchian,

H. P.; Cross, J. B.; Adamo, C.; Jaramillo, J.; Gomperts, R.; Stratmann, R. E.; Yazyev, O.; Austin, A. J.; Cammi, R.; Pomelli, C.; Ochterski, J. W.; Ayala, P. Y.; Morokuma, K.; Voth, G. A.; Salvador, P.; Dannenberg, J. J.; Zakrzewski, V. G.; Dapprich, S.; Daniels, A. D.; Strain, M. C.; Farkas, O.; Malick, D. K.; Rabuck, A. D.; Raghavachari, K.; Foresman, J. B.; Ortiz, J. V.; Cui, Q.; Baboul, A. G.; Clifford, S.; Cioslowski, J.; Stefanov, B. B.; Liu, G.; Liashenko, A.; Piskorz, P.; Komaromi, I.; Martin, R. L.; Fox, D. J.; Keith, T.; Al-Laham, M. A.; Peng, C. Y.; Nanayakkara, A.; Challacombe, M.; Gill, P. M. W.; Johnson, B.; Chen, W.; Wong, M. W.; Gonzalez, C.; Pople, J. A.; Gaussian 03 Revision B04; Gaussian, Inc.: Pittsburgh, PA, 2003.

31. Scott, A. P.; Radom, L. Harmonic Vibrational Frequencies: An Evaluation of Hartree-Fock, Moller-Plesset, Quadratic Configuration Interaction, Density Functional Theory, and Semiempirical Scale Factors. *J. Phys. Chem.* **1996,** *100,* 16502.
32. Gronert, S.; Merrill, G. N.; Kass, S. R. Fluoride-Induced Elimination of Ethyl Fluoride. The Importance of High-Level Optimizations in ab Initio and DFT Studies. *J. Org. Chem.* **1995,** *60,* 488.
33. Schlosser, A.; Lehmann, W. D. Five-Membered Ring Formation in Unimolecular Reactions of Peptides: A Key Structural Element Controlling Low-Energy Collision-Induced Dissociation of Peptides. *J. Mass Spectrom.* **2000,** *35,* 1382.